2014 IEEE International Conference on Robotics & Automation (ICRA)
Hong Kong Convention and Exhibition Center
May 31 - June 7, 2014. Hong Kong, China

Contact Event Detection for Robotic Oil Drilling

X. Alice Wu[1], Natalie Burkhard[1], Barrett Heyneman[1], Roald Valen[2], and Mark Cutkosky[1]
[1]The Center for Design Research – Stanford University – Stanford, CA 94305–2232, USA
[2]Robotic Drilling Systems™AS – Sandnes, Norway

***Abstract*— To ensure safe and reliable operation in a robotic oil drilling system, it is essential to detect contact events such as impacts and slips between end-effectors and workpieces. In this challenging application, where high forces are used to manipulate heavy metal pipes in noisy environments, acoustic emissions (AE) sensors offer a promising contact sensing solution. Real-time AE signal features are used to create a multinomial contact event classifier. The sensitivity of signal features to a variety of contact events including two types of slip is presented. Results indicate that the classifier is able to robustly and dynamically classify contact events with >90% accuracy using a small set of AE signal features.**

***Index Terms*— contact sensing, slip, manipulation, acoustic emissions**

I. Introduction

Robotic drilling has become an increasingly desirable goal as the oil industry seeks to enhance operator safety and reduce costs. Robotic Drilling Systems AS (RDS) has developed an autonomous rig for unmanned exploration drilling in harsh environments. Contact and slip event detection is an important capability for reliable robotic manipulation, enabling quick and appropriate reaction to unanticipated events. This paper addresses unintentional slips between robotic end effectors (grippers and roughnecks) and their payloads: large, heavy metal pipes (Fig. 1). This is a challenging new robotics application for which no prior solutions exist.

Numerous robotic slip detection methods exist, many of which rely on detecting minute displacements between an end effector and payload using mechanical, optical, magnetic or even thermal transducers. Bio-inspired methods often measure the vibrations or rapid changes in contact stress that accompany incipient slips. These dynamic sensing approaches have the advantage of allowing response before noticeable movement occurs [1,2]. Recent reviews of contact and slip sensing are found in [3]–[5].

For robotic drilling applications, sensor placement at the contact interface is impossible due to hazardous conditions including high temperatures and pressures as well as explosion risks. The presented scheme demonstrates the ability to identify contact events using non-colocated acoustic emissions (AE) sensing. Early investigations [6,7] indicated that AE is sensitive to slip between metal grippers and workpieces, inspiring the approach presented here. Unlike conventional robotic tactile sensors, AE transducers can be easily packaged to withstand harsh environments. In addition, AE signals typically occur at frequencies over 100 kHz, well above common low-frequency noise sources.

This paper describes the application of AE signal analysis to detect and distinguish various contact events such as slips and impacts. The next section reviews AE sensing, focusing on signal features likely to be effective for such a classification problem. The subsequent section describes the signal processing method and event classification scheme. Experiments, initially using a benchtop apparatus and ultimately the full-scale RDS robotic gripper, are described and results presented, followed by conclusions and further work.

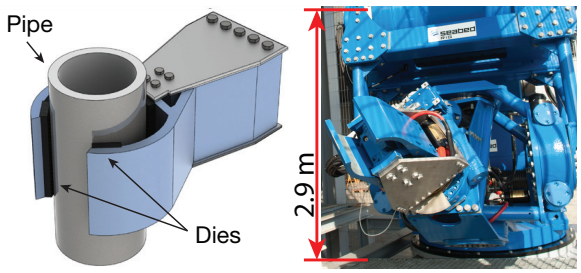

(a) Robotic gripper

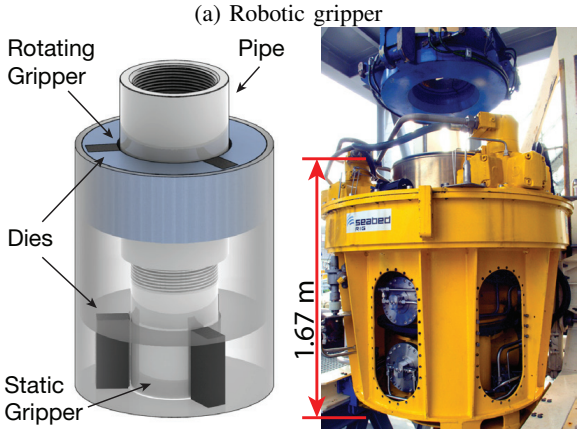

(b) Roughneck for mating pipes

Fig. 1: Robotic Drilling System pipe handling devices

II. Acoustic Emissions Sensing

A. AE Generation and Detection

The interaction of steel components generates stress waves called *accoustic emissions* (AE). Asperity contact is the primary source [8] with contributions from plastic deformation, fracture, impulsive shock, and micro-vibration [9,10]. AE signal analysis is an established tool for monitoring metal-working processes and the structural health of metal assemblies [9,10]. Advantages of AE include a direct correlation with the amount of metal deformation or fracture and a high signal to noise ratio [9,11,12].

As AE waves travel through a structure, material heterogeneities and component interfaces attenuate the signal [9, 11,13]. Thus, AE is typically measured using collocated piezoelectric transducers mounted near the source of plastic deformation [7,14]. A vibration couplant grease is often applied between the AE sensor and its mount to improve transmission. Measured AE signals consist of "hits", or bursts of activity for which the signal magnitude is above some threshold.

In the present application, contact events among grippers, pipes, and external objects all generate AE. A single event can generate many AE hits, each of which has signal features that may be extracted for pattern classification. Contact conditions significantly affect AE signals [7,11,14,15], a feature exploited here to distinguish between contact events.

B. Event Classification Techniques

Various supervised and unsupervised pattern recognition techniques have been applied to AE signals for manufacturing and structural monitoring applications [16,17]. Supervised learning methods range from simple classifiers such as k-nearest neighbors (k-NN) [18] to more sophisiticated back-propagation neural networks [19] and support vector machines (SVM) [20,21]. If prior knowledge regarding event classes is unavailable, unsupervised classifiers can be used to perform event classification. Some methods proposed for AE data analysis include max-min distance, cluster seeking, k-means, and isodata [22,23]. In both supervised and unsupervised cases, prior work has demonstrated the ability to distinguish between different types of AE events [24]. To the authors' knowledge, such real-time AE features have not previously been used for classifying robotic contact events.

III. Methods

A. Contact Event Definitions

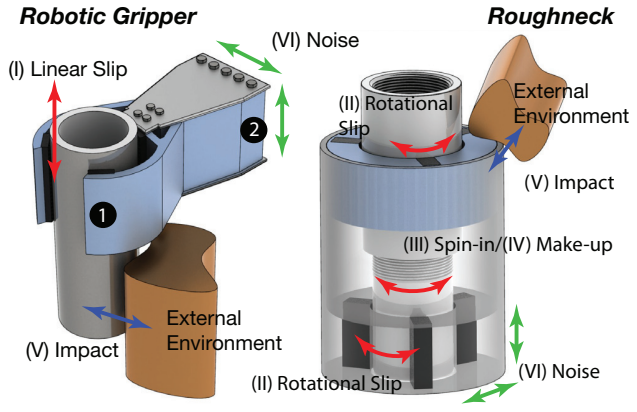

Fig. 2: Contact events classes for the robotic gripper and roughneck. Labels 1 and 2 represent sensor placement locations on the robotic gripper setup detailed in Section IV-B

The system manipulates pipes with a robotic gripper and a roughneck (Fig. 1). Both the gripper and roughneck grasp steel pipes with hardened steel dies. Contact events (including impacts, slips, and other unspecified sources of noise) may occur at either site.

The robotic gripper's primary function is to transfer pipes and move them into or out of the roughneck. During pipe transfer and placement, slips may occur along the pipe's axis. However, rotational slips about the pipe's long axis are unlikely. Contact event classes for the gripper are: (I) linear slip, (V) impact, and (VI) noise (Fig. 2).

The roughneck has two sets of jaws that grip pipes in a manner similar to a lathe chuck. Its primary function is to connect sections of pipe by screwing or threading them together. Pipe threading has two stages: *spin-in* and *make-up*. During spin-in, the rotating upper jaw grips the upper pipe and spins at 100 RPM, applying torques ranging from 2-3 kNm, while the lower jaws hold the bottom pipe stationary. If spin-in is successful, the pipe mating process culminates with a make-up operation, slowly rotating the upper pipe a bit further with a torque of 20-60 kNm. Slips are possible at the upper and lower jaw contacts. In addition, intentional slips occur between the threads of the upper and lower pipes during spin-in and make-up. Both the intentional and unintentional slips involve plastic deformation and generate AE signals. However, it is important to differentiate them because unintentional slips represent a process failure. External impact events are also possible during this process, therefore the contact events for the roughneck are: (II) rotational slip, (III) spin-in threading, (IV) make-up threading, (V) impact, and (VI) noise.

B. Sensor Features Implementation

1) Data Acquisition and Postprocessing: Two wideband integral preamplifier sensors (MISTRAS, Model WDI-AST) with gains of 40dB and response frequencies 200-900 kHz were used to capture AE signals at a hit length of 1.28 ms. A PCI-2 Based AE System (MISTRAS) was used to sample the signals. In practice, the sensors also captured signals in the 50-100 kHz range.

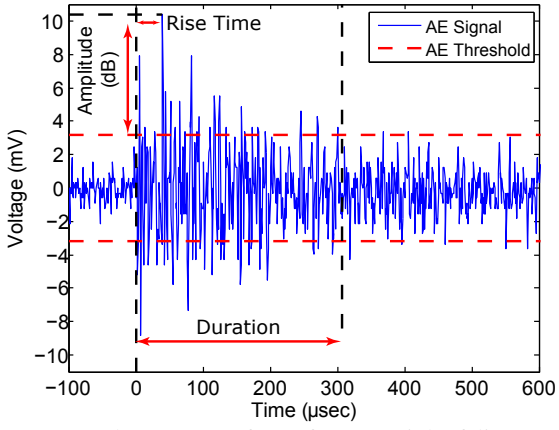

Fig. 3: Sample AE waveform from a trial of linear slip on the benchtop setup

The accompanying data acquisition software outputs a set of real-time, distinct AE sensor features in both the time and frequency domains. Fig. 3 illustrates the measurement principles of AE used to calculate the features. Frequency features require performance of a real-time FFT. Feature categories with a large dynamic range were normalized,

TABLE I: AE Sensor Feature Set

#	Sensor Feature	Interpretation	Positively Correlated Conditions	Contact Events
1	Amplitude (AMP)	maximum (+/-) AE signal excursion during an AE hit (dB)	wear volume or plowing action [25]	grinding (I, II)
2	Average signal level (ASL)	averaged AE amplitude (dB)	load, speed, asperity contact, wear, friction, wear rate [6,7,10,12,25,26]	grinding, gripping (I, II), fast slip (V, VI)
3	Frequency centroid (FREQ-C)	sum of amplitude-weighted frequencies divided by amplitude sum (kHz)	speed, asperity contact, contact area length in sliding direction [14,27,28]	fast, long-distance sliding, large contact area (V, VI)
4-7	Partial powers, 4 bins (FREQPP1-4)	fraction of power spectrum in a specified frequency range (%)	sliding speed, friction coefficient [28]	fast slip (V, VI)

including amplitude (AMP) and average signal level (ASL). Data from both sensors were used for the event classifier.

Feature selection is key to successful pattern recognition methodology. As noted in Section II, prior work has shown correlations between AE features and various contact phenomena. Based on these findings, 7 of the 19 software-generated features were selected for event classification (see Table I). Performance results are presented in Section V.

C. Contact Event Classifier

The contact event sets for the classifier are modeled as multinomial distributions [29] with nominal labels assigned to each event class. Model fitting on AE features was performed using WEKA 3.7 [30], and the response model was calculated in MATLAB. Although prior art has demonstrated good multi-class event classification results using Gaussian discriminant analysis (GDA) [16]. GDA was developed for normally distributed explanatory variables and is appropriate when normality assumptions are fulfilled. However, here the predictor data distribution is unknown, making a multinomial logistic regression the more robust choice because the latter makes fewer assumptions regarding underlying data [31]. The multinomial logistic regression model is given below.

Given n instances of k contact event types and f features, the calculated parameter matrix B is an $f \times (k-1)$ matrix. Let β_j be the j-th column of B. The nominal reponse model P_j, or the probability of outcome y being event type j given sensor feature vector x of length f, is:

$$P_j(x^{(i)}) = \frac{e^{\beta_j^T x^{(i)}}}{1 + \sum_{j=1}^{k-1} e^{\beta_j^T x^{(i)}}} \quad \text{for} \quad \begin{cases} i = 1, \cdots, n \\ j = 1, \cdots, k-1 \end{cases} \tag{1}$$

Equivalently, for a set of f features (k is the last event class):

$$ln\left(\frac{P_j(x^{(i)})}{P_k(x^{(i)})}\right) = \beta_j^T x^{(i)} = \beta_{j(0)} + \beta_{j(1)} x_1^{(i)} + \beta_{j(2)} x_2^{(i)} + \cdots \tag{2}$$

The last event class k has the probability:

$$P_k(x^{(i)}) = 1 - \sum_{j=1}^{k-1} P_j(x^{(i)}) = \frac{1}{1 + \sum_{i=1}^{k-1} e^{\beta_j^T x^{(i)}}} \tag{3}$$

Each AE hit is classified as the event with the highest probability value. The algorithm was trained and tested using 70/30 holdout on both the benchtop and RDS robotic gripper devices. Parameters for the robotic gripper and the roughneck event sets were trained separately.

IV. Experiments

A. Benchtop Setup (Stanford, CA)

1) Apparatus: The benchtop setup (Fig. 4) has a 25.4 mm steel pipe gripped by a bench yoke vise (RIDGID) mounted to an aluminum frame. The vise jaws have three hardened-steel dies with standard oil-drilling profiles. A 7 kN thrust, linear actuator (ServoCity) was mounted to the frame. On RDS's robotic gripper, the AE sensors cannot be mounted directly to the pipes, dies, or gripper jaws. In order to mimic this constraint, in the benchtop setup the AE sensors were mounted on steel plates mounted between the bottom dies and the vise body, with couplant grease applied at all interfaces between sensors, plates, and dies. A force load cell was mounted between the top die and the vise yoke, and a witness LVDT sensor was aligned with the actuator.

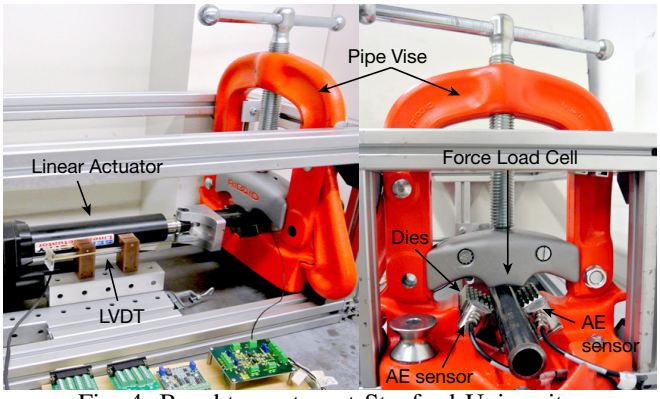

Fig. 4: Benchtop setup at Stanford University.

2) Procedure: 32 experiments were used to generate AE data: 6 trials of (I) linear slip, 3 of (II) rotational slip, 3 of (III) spin-in, 2 of (IV) make-up, 12 of (V) impact, and 6 of (VI) noise. The linear actuator produced linear slip by pushing the pipe through the clamped vise jaws. All other contact events were performed manually. Impacts involved striking the pipe, vise, or frame with a dead blow mallet or a metal hammer. Low-frequency noise was introduced by attaching vibration motors to various parts of the system. Note that although the linear actuator produces a controlled linear motion, the slip phenomenon we are attempting to detect are uncontrollable by definition. So long as there is

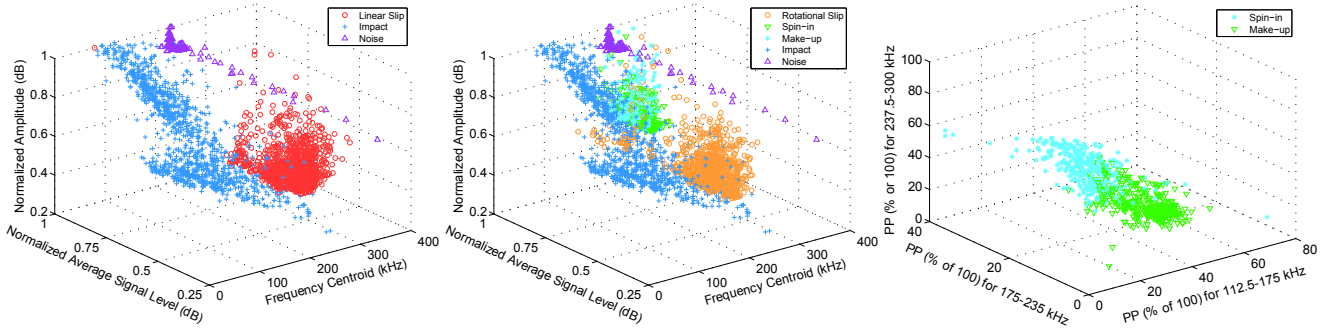

(a) Robotic gripper event space (b) Roughneck event space (c) Roughneck event subspace

Fig. 5: Benchtop results visualization

steel-on-steel interaction, AE signals can be recorded and further characterized based on signal features and not the means by which the signals are produced. The LVDT tracked linear pipe displacement, and the load cell collected grip force levels. Note that on this setup, the grip force is not actively maintained throughout each trial, it is set only by the initial tightening of the vise. Grip forces during slip ranged from 600 N to 1.5 kN. Data were sampled at 1 MHz and processed with AE threshold set at 30 dB. AE magnitudes are similar to those obtained on gripper as noted in the next section.

B. Robotic Gripper (Sandnes, Norway)

1) Apparatus: RDS's apparatus has a hydraulic linear actuator and a robotic gripper capable of 25.8 kN of grip force with three sets of steel dies. Experiments were performed using a 253 mm pipe. The same AE sensors were attached to various locations on the gripper, with couplant grease at the interface (Fig. 6). Grip force was held constant throughout each trial via closed-loop control.

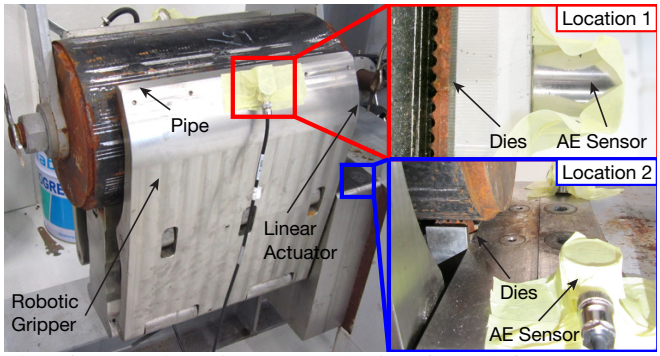

Fig. 6: Robotic gripper. Clockwise from left: apparatus, sensor near slip interface/top dies, sensor near bottom dies.

2) Procedure: The same gripper contact events (I) linear slip, (V) impact, and (VI) noise (Fig. 2) were tested. Linear slip and impact trial protocols were unchanged with respect to the benchtop apparatus. Noise was introduced via hydraulic servo valves mounted on the system's frame. Two locations were tested (Fig. 6): location 1 is analogous to the benchtop setup in terms of AE coupling, location 2 is RDS's desired sensor placement location, as location 1 is within a hazardous "red zone". At each location, three trials were conducted for impact, noise, and linear slip at two force levels (2.7 kN and 8.1 kN). These trials were used to train and test the classifier.

Additional multi-event sequence trials at the two grip force levels were also conducted. These tests involved a sequence of continuous contact events. For these experiments, AE threshold was raised to 35 dB due to baseline noise levels.

V. Results

A. Benchtop Results

1) Sensor Feature Visualization: Visualization of three features (frequency centroid, normalized AMP, normalized ASL) demonstrates qualitatively the separation of event classes into distinct populations (Fig. 5). While gripper events have excellent separation among event classes, roughneck events show good distinction for (II) rotational slip, (V) impact, and (VI) noise while (III) spin-in and (IV) make-up overlap. Plotting three other features visually distinguishes (III) and (IV) (Fig. 5c).

2) Event Classifier Performance: For hold-out validation, the algorithm is accurate and robust (Tables II and III) for accuracy (acc), specificity (spec), and sensitivity (sens). For robotic drilling applications, sensitivity is crucial because it reflects false negative rates (FNR). A false negative indicates slip occurred but was not accurately identified as such. High sensitivity is indicative of low FNR. The robotic gripper classifier demonstrated accuracy above 97%, and FNR was highest for impact. The roughneck classifier demonstrated accuracy above 90%, and FNR was again highest for impact. Note that each event class contains AE data from multiple experimental trials.

TABLE II: Benchtop classifier performance: Robotic Gripper

Class	Training Samples	Class Label I	V	VI	Acc. (%)	Sens. (%)	Spec. (%)
(I) Linear Slip	2148	919	2	0	97.5	99.8	92.9
(V) Impact	778	32	303	0	97.5	90.5	99.8
(VI) Noise	302	1	0	129	99.9	99.2	100.0

TABLE III: Benchtop classifier performance: Roughneck

Class	Training Samples	Class Label II	III	IV	V	VI	Acc. (%)	Sens. (%)	Spec. (%)
(II) Rotational Slip	839	328	1	14	18	0	91.6	90.9	92.0
(III) Spin-in	244	0	98	1	6	0	96.9	93.3	97.3
(IV) Make-up	235	2	3	96	1	0	97.5	94.1	97.9
(V) Impact	778	52	21	4	258	0	90.1	77.0	96.4
(VI) Noise	302	0	0	1	0	129	99.9	99.2	100.0

B. RDS Robotic Gripper Results

1) Sensor Feature Visualization: Visualizing the same three features for the RDS robotic gripper also shows excellent event separation at locations 1 and 2. Normalized amplitude levels for (I) linear slip are lower at location 2 than location 1, while the overall distributions at both locations are similar to the distribution for the same event class on the benchtop setup.

2) Event Classifier Performance: For hold-out validation, the algorithm is still accurate and robust (Tables IV and V). Location 2 is particularly important because it is the ideal sensor location in practice, although location 1 is more analogous to the benchtop setup and closest to the slip source. At location 1, the classifier demonstrated accuracy above 97%, and FNR was again highest for impact. The location 2 classifier also demonstrated accuracy above 97%, but FNR was highest for linear slip. This difference may be attributed to signal attenuation due to remote sensor location.

TABLE IV: RDS Classifier Performance: Location 1

Class	Training Samples	Class Label I	V	VI	Acc. (%)	Sens. (%)	Spec. (%)
(I) Linear Slip	511	213	5	2	97	96.8	97.5
(V) Impact	166	2	68	2	97	94.4	97.8
(VI) Noise	16	0	0	8	98.7	100.0	98.6

TABLE V: RDS Classifier Performance: Location 2

Class	Training Samples	Class Label I	V	VI	Acc. (%)	Sens. (%)	Spec. (%)
(I) Linear Slip	147	57	7	0	97.0	89.1	99.2
(V) Impact	129	2	54	0	97.0	96.4	97.1
(VI) Noise	412	0	0	178	100.0	100.0	100.0

3) Performance on Multi-event Sequences: Fig. 8 demonstrates classifier performance over a finite time period during which various contact events were performed. The algorithm successfully detected all events and performed a classification. Each event had numerous associated hits, and the vast majority of each event's hits were correctly classified. During the test sequence shown in Fig. 8a, the system was impacted at 0 s, and two long slip events occurred at 16 and 26 s. For this sequence, classifier accuracy was 93.1%. The test sequence in Fig. 8b consists of three short slip events at 5, 12, and 15 s followed by impacts at 18 and 27 s. For this sequence, classifier accuracy was 95.8%. Performance is visualized in Fig. 8.

C. Witness Sensor Slip Validation

To validate linear slip conditions on the benchtop setup, a LVDT sensor served as a witness sensor for linear displacement. As expected, plastic deformation of steel increases with slip and generates increasing numbers of AE hits. On average, eight AE hits were detected and classified within 1 mm of displacement. For robotic oil drilling, slips of less than 2 mm are not significant.

VI. Discussion

A. Contact Event Classifier

The choice of reference class k in the multinomial regression is important for performance as the probability constraint on the multinomial regression classifier calculates weights only for the first $k-1$ events. Here, classifier performance was best when (VI) noise was the reference event. Normalization of certain AE sensor features such as amplitude and ASL was found to improve classification accuracy over non-normalized features, primarily due to numerical precision when calculating feature weights β_j.

In addition to high accuracy and robustness, the classifier demonstrates the potential for realtime implementation (with offline model parameter fitting). Using the MATLAB profiler (5000 executions, 1ms clock precision, 2 GHz clock speed) on standard Windows 7 OS without any code optimization, our classifier executes in 1ms per AE hit on average.

B. Validated AE Conditions

Results demonstrate the utility of AE signal analysis as a contact event detection tool for robotic manipulation. The classifier demonstrates high performance for both a benchtop setup and RDS's robotic gripper for oil drilling. Differences between the two setups include physical scale, noise sources (and consequent AE threshold), associated system artifacts, magnitude of grip forces, and the number of mechanical interfaces between the slip location and the sensor.

Prior art in AE sensing primarily uses direct coupling, which is impossible to achieve for this application. On both setups, results indicate the ability to detect contact events using non-collocated AE sensors mounted a few mechanical connections away from the source of AE signals. The benchtop setup had couplant grease at all interfaces for vibrational coupling while the robotic gripper setup only had couplant grease at the sensor mounting location. Enhanced vibrational coupling in the robotic gripper could increase performance.

Knowledge of known noise sources at sensor resonance aids classifier performance. RDS requires sensor placement at location 2 (Fig. 6). Initially, servo valves were attached to the frame and introduced high magnitude noise (80 dB) at the AE sensor resonance (125 kHz). Because this noise source was located much closer to location 2 than location 1, the noise overwhelmed slip signals at location 2 and led to poor classifier performance. Classifier performance was excellent when the valves were relocated. To mitigate such effects in practice, filtering via software or using narrowband AE sensors could also suffice.

VII. Conclusions

An accurate and robust method has been presented for detecting contact events between grippers and workpieces for robotic oil drilling. The method uses acoustic emissions (AE) and, for each burst or "hit" of AE signal, uses features of the AE signal to determine probabilities for each of a set of possible contact events. This is a new approach to contact event sensing and classification in an environment that most other robotic tactile sensors cannot survive.

Traditional AE sensing applications mount a sensor on or immediately adjacent to a workpiece. However, in oil drilling it is infeasible to attach sensors directly to the pipes or even to the jaws of the grippers that handle them. Results

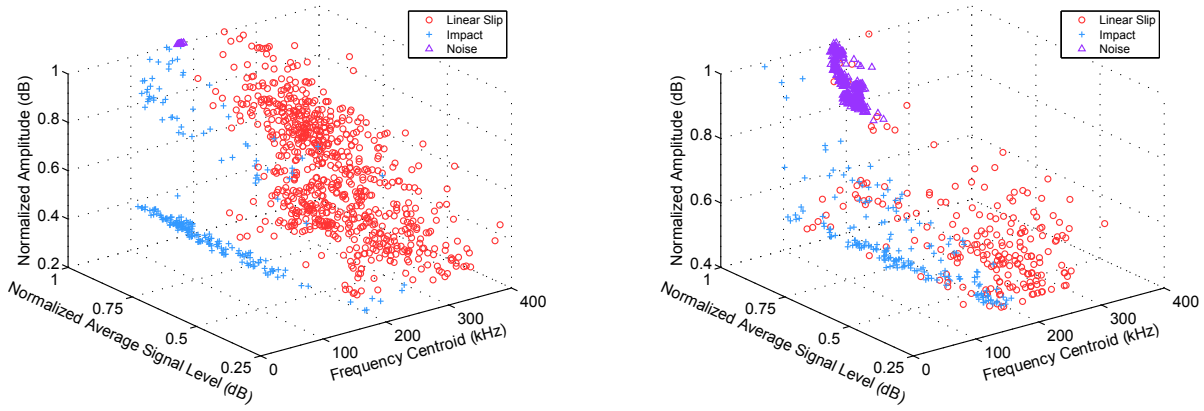

(a) Location 1 event space

(b) Location 2 event space

Fig. 7: RDS Robotic gripper visualization

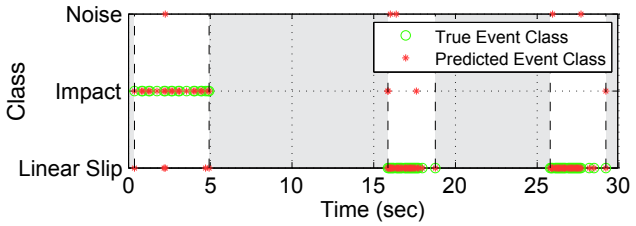

(a) Contact event sequence with sensor at location 1

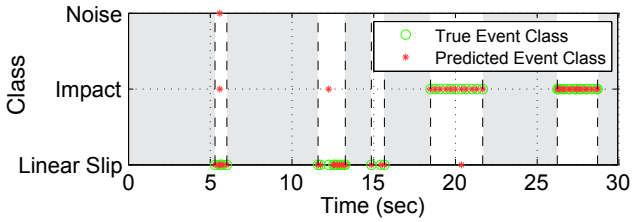

(b) Contact event sequence with sensor at location 2

Fig. 8: Contact event classification over time. Locations 1 and 2 indicate experimental sensor placement. Gray regions indicate time periods where no events took place.

presented here indicate that coupling the AE sensors close to the location of interest, but not directly at the source of contact, nonetheless allows accurate identification of multiple contact events.

VIII. Future Work

This work is part of a broader goal to develop a state monitoring system for robotic oil drilling. The goal of such a system is to determine whether the suite of sensor information at each instant is consistent with normal programmed operation.

Use of multiple sensors may aid event identification through source location. For example, signal coherence among neighboring sensors may allow the discrimination of incipient slip occurring at different contact interfaces [32]. Identification of additional contact events is also possible if their AE signal features are distinct, a condition satisfied if the contact conditions are also distinct.

Utilizing contextual information may improve the classifier robustness [33]. Contextual information captures *a priori* system knowledge and may logically exclude events or raise/lower the confidence that a particular event is occurring. Examples of contextual information that may exclude certain events include pipe presence and sensor location; if a pipe is absent, slip events (I-IV) cannot occur. Contextual features with more complex distributions may incorporate visual or audible sensor information, human feedback, or grip force information. Implementation would involve assigning a confidence distribution function to these context features and evaluating them for each contact event. Each contact event probability the multinomial regression produces would then be multiplied by these values.

Using time history may also prove beneficial. A single contact event typically generates multiple AE hits. In this work, each hit is classified individually because the number of hits per event has not been investigated. However, if a particular event type has been assigned to a series of hits, the probability of the same event increases for subsequent hits within a short time period.

IX. Acknowledgements

We thank Svein Søyland, Vegard Voll and the rest of the RDS team for assistance on the robotic gripper experiments, Ron Miller from the MISTRAS Group Inc. for technical support on AE sensing, Andrew Maas and Lucas Janson for statistical advice. This work was supported by the Robotic Drilling Systems AS (Norway). Alice Wu is supported in part by the NSF Graduate Research Fellowship. Natalie Burkhard is supported in part by the Stanford Graduate Research Fellowship.

References

[1] M. Tremblay and M. R. Cutkosky, "Estimating friction using incipient slip sensing during a manipulation task," in *IEEE International Conference on Robotics and Automation*, pp. 429–434, IEEE, 1993.

[2] J. M. Romano, K. Hsiao, G. Niemeyer, S. Chitta, and K. J. Kuchenbecker, "Human-inspired robotic grasp control with tactile sensing," *Robotics, IEEE Transactions on*, vol. 27, no. 6, pp. 1067–1079, 2011.

[3] M. R. Cutkosky, R. Howe, and W. Provancher, "Force and Tactile Sensors," in *Springer Handbook of Robotics*, pp. 455–476, 2008.

[4] R. S. Dahiya, G. Metta, M. Valle, and G. Sandini, "Tactile sensing—from humans to humanoids," *Robotics, IEEE Transactions on*, vol. 26, no. 1, pp. 1–20, 2010.

[5] M. Cutkosky and J. Ulmen, "Dynamic Tactile Sensing," in *The Human Hand: a source of inspiration for robotic hands* (B. Balasubramanian and V. Santos, eds.), ch. 18, Springer-Verlag, in press ed., 2013.

[6] D. Dornfeld and C. Handy, "Slip detection using acoustic emission signal analysis," 1987.

[7] S. Rangwala, F. Forouhar, and D. Dornfeld, "Application of acoustic emission sensing to slip detection in robot grippers," *International Journal of Machine Tools and Manufacture*, vol. 28, pp. 207–215, Jan. 1988.

[8] R. Boness and S. McBride, "Adhesive and abrasive wear studies using acoustic emission techniques," *Wear*, vol. 149, pp. 41–53, Sept. 1991.

[9] D. Mba and R. Rao, "Development of Acoustic Emission Technology for Condition Monitoring and Diagnosis of Rotating Machines; Bearings, Pumps, Gearboxes, Engines and Rotating," *The Shock and Vibration Digest*, vol. 38, no. 1, pp. 3–16, 2006.

[10] J. Sun, R. Wood, L. Wang, I. Care, and H. Powrie, "Wear monitoring of bearing steel using electrostatic and acoustic emission techniques," *Wear*, vol. 259, pp. 1482–1489, July 2005.

[11] J. Sikorska and D. Mba, "AE Condition Monitoring: Challenges and Opportunities," *Engineering asset management*, pp. 1–12, 2006.

[12] C. K. Tan, P. Irving, and D. Mba, "A comparative experimental study on the diagnostic and prognostic capabilities of acoustics emission, vibration and spectrometric oil analysis for spur gears," *Mechanical Systems and Signal Processing*, vol. 21, pp. 208–233, Jan. 2007.

[13] J. Miettinen and V. Siekkinen, "Acoustic emission in monitoring sliding contact behaviour," *Wear*, vol. 183, pp. 897–900, 1995.

[14] V. Baranov, E. Kudryavtsev, and G. Sarychev, "Modelling of the parameters of acoustic emission under sliding friction of solids," *Wear*, vol. 202, pp. 125–133, Jan. 1997.

[15] K. Asamene and M. Sundaresan, "Analysis of experimentally generated friction related acoustic emission signals," *Wear*, vol. 296, pp. 607–618, Aug. 2012.

[16] R. Miller, E. Hill, and P. Moore, *Acoustic Emission Testing*. Nondestructive Testing Handbook, American Society for Nondestructive Testing, 2005.

[17] E. Kannatey-Asibu and E. Emel, "Linear Discriminant Function Analysis of Acoustic Emission Signals for Cutting Tool Monitoring," *Mechanical Systems & Signal Processing*, vol. 1, no. 4, pp. 333–347, 1987.

[18] K. Ono and Q. Huang, "Pattern recognition analysis of acoustic emission signals," *NDT & E International*, vol. 30, no. 2, pp. 109–109, 1997.

[19] E. Hill, J. Iizuka, I. Kaba, H. Surber, and Y. Poon, "Neural network burst pressure prediction in composite overwrapped pressure vessels using mathematically modeled acoustic emission failure mechanism data," *Research in Nondestructive Evaluation*, vol. 23, no. 2, pp. 89–103, 2012.

[20] N. Ince, C.-S. Kao, M. Kaveh, A. Tewfik, and J. Labuz, "A Machine Learning Approach for Locating Acoustic Emission," *EURASIP Journal on Advances in Signal Processing*, vol. 2010, no. 1, 2010.

[21] Y. Yu and L. Zhou, "Acoustic emission signal classification based on support vector machine," *TELKOMNIKA Indonesian Journal of Electrical Engineering*, vol. 10, no. 5, pp. 1027–1032, 2012.

[22] A. Anastassopoulos and T. Philippidis, "Clustering methodology for the evaluation of acoustic emission from composites," *Journal of acoustic emission*, vol. 13, no. 1-2, pp. 11–22, 1995.

[23] A. Anastassopoulos, D. Kouroussis, and A. Tsimogiannis, "Unsupervised Classification of Acoustic Emission Sources from Aerial Man Lift Devices," in *World Conference on NDT-15th. Roma, Italy*, 2000.

[24] N. Godin, S. Huguet, R. Gaertner, and L. Salmon, "Clustering of acoustic emission signals collected during tensile tests on unidirectional glass/polyester composite using supervised and unsupervised classifiers," *NDT & E International*, vol. 37, pp. 253–264, June 2004.

[25] C. Jiaa and D. Dornfeld, "Experimental studies of sliding friction & wear via acoustic emission signal analysis," *Wear*, vol. 139, pp. 403–424, 1990.

[26] Y. Fan, F. Gu, and A. Ball, "Modelling acoustic emissions generated by sliding friction," *Wear*, vol. 268, pp. 811–815, Feb. 2010.

[27] S. Rangwala and D. Dornfeld, "A study of acoustic emission generated during orthogonal metal cutting—2: spectral analysis," *International journal of mechanical sciences*, vol. 33, no. 6, pp. 489–499, 1991.

[28] G. Sarychev and V. Shchavelin, "Acoustic emission method for research and control of friction pairs," *Tribology International*, vol. 24, pp. 11–16, Feb. 1991.

[29] J. le Cessie, S., van Houwelingen, "Ridge Estimators in Logistic Regression," *Applied Statistics*, vol. 4, no. 1, pp. 192–201, 1992.

[30] M. Hall, H. National, E. Frank, G. Holmes, B. Pfahringer, P. Reutemann, and I. H. Witten, "The WEKA Data Mining Software : An Update," *SIGKDD Explorations*, vol. 11, no. 1, pp. 10–18, 2009.

[31] S. J. Press and S. Wilson, "Choosing between logistic regression and discriminant analysis," *Journal of the American Statistical Association*, vol. 73, no. 364, pp. 699–705, 1978.

[32] B. Heyneman and M. R. Cutkosky, "Slip Interface Classification through Tactile Signal Coherence," in *IEEE/RSJ International Conference on Intelligent Robots and Systems (IROS)*, 2013.

[33] M. Tremblay and M. R. Cutkosky, "Using sensor fusion and contextual information to perform event detection during a phase-based manipulation task," *Proceedings 1995 IEEE/RSJ International Conference on Intelligent Robots and Systems. Human Robot Interaction and Cooperative Robots*, vol. 3, pp. 262–267, 1995.